



PCP and POCOP complexes of calcium†

Cite this: *Chem. Commun.*, 2025, 61, 7827

Alessandro Messori,^{‡a} Marcel Potocnik,^{‡a} Sara Belazregue,^a Richard Collins,^{id a} Tobias Krämer^{id b} and F. Mark Chadwick^{id *a}

Received 17th February 2025,
Accepted 26th March 2025

DOI: 10.1039/d5cc00872g

rsc.li/chemcomm

The first synthesis of PCP and POCOP complexes of calcium are described. $\text{Ca}(\text{N}(\text{SiMe}_3)_2)_2$ is reacted with $\text{Li}[(^t\text{Bu})\text{PCP}]$ or $\text{Li}[(^t\text{Bu})\text{POCOP}]$ to form $(^t\text{Bu})\text{PCP}\text{Ca}(\text{N}(\text{SiMe}_3)_2)_2$ (**1a**) and $(^t\text{Bu})\text{POCOP}\text{Ca}(\text{N}(\text{SiMe}_3)_2)_2$ (**1b**). Reaction of **1b** or $\text{Ca}(\text{N}(\text{SiMe}_3)_2)_2$ with excess $\text{Li}[(^t\text{Bu})\text{POCOP}]$ leads to a homoleptic complex $(^t\text{Bu})\text{POCOP}_2\text{Ca}$, **2**. The $(^i\text{Pr})\text{POCOP}$ ligand exclusively forms the homoleptic complex $(^i\text{Pr})\text{POCOP}_2\text{Ca}$, **3**.

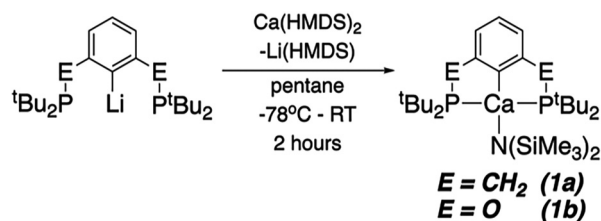
In comparison to transition metals, the organometallic chemistry of the alkaline-earth metals has been severely neglected. Due to both their perceived lack of redox activity and their electropositive nature, their chemistry has often been relegated to use as synthons for the more popular transition metals, most notably as Grignard reagents.^{1,2} However, recent awareness of the sustainability issues surrounding metals commonly used in catalysis has brought the spotlight onto the more earth abundant metals, and particularly those of group 2.³

In the last couple of decades, the alkaline-earth metals' chemistry has been further developed. Groups have developed polymerisation, hydroamination and hydrosilylation catalysis using these metals.^{3–7} Calcium has been deployed into the field of small molecule activation, including CO homologation, the reduction of benzene and N_2 activation.^{8–10} Though group 2 pincer complexes have recently been used for hydrogenation chemistry, the chemistry is dominated by the use of the β -diketimide 'nacnac' ligand.¹¹ Since Chisholm's breakthrough paper in 2004, the simple (nacnac)Ca fragment has been the feature of over 100 papers.^{12–15} We recently developed a route to $^{\text{R}}\text{PCP}\text{M}$ complexes that precludes the traditional requirement of oxidative addition – this ligand shares some of

the 'nacnac' ligand's primary features (monoanionic, ease of installation of bulk close to the metal centre) whilst retaining useful differences (e.g. tridentate vs. bidentate).^{16,17} We therefore wished to investigate whether it was possible to make $^{\text{R}}\text{PCP}/^{\text{R}}\text{POCOP}$ calcium complexes ($^{\text{R}}\text{PCP} = 2,6-(\text{R}_2\text{PCH}_2)_2\text{C}_6\text{H}_3$; $^{\text{R}}\text{POCOP} = 2,6-(\text{R}_2\text{PO})_2\text{C}_6\text{H}_3$). To date there are only two reports of group 2 $^{\text{R}}\text{PCP}$ complexes (both reporting a $(^{\text{R}}\text{PCP})_2\text{Mg}$ fragment),^{18,19} and there are no reports of group 2 $^{\text{R}}\text{POCOP}$ complexes. Previous attempts to make $(^{\text{R}}\text{PCP})\text{Ca}$ complexes resulted in a mixture of products which cleaved the P–C bonds.¹⁸ Very recently, Milstein has developed a route to anionic 'PNP' pincer complexes of calcium, which showed interesting small molecule reactivity with N_2O .²⁰ Herein, we report the formation of the first $^{\text{R}}\text{PCP}$ and $^{\text{R}}\text{POCOP}$ Ca complexes.

Both $(^t\text{Bu})\text{PCP}\text{Ca}(\text{HMDS})_2$ ($(^t\text{Bu})\text{PCP} = 2,6-(^t\text{Bu}_2\text{PCH}_2)_2\text{C}_6\text{H}_3$; $\text{HMDS} = \text{N}(\text{SiMe}_3)_2$, **1a**) and $(^t\text{Bu})\text{POCOP}\text{Ca}(\text{HMDS})_2$ ($(^t\text{Bu})\text{POCOP} = 2,6-(^t\text{Bu}_2\text{PO})_2\text{C}_6\text{H}_3$, **1b**) can be made by analogous routes (Scheme 1). The appropriate lithium precursor is reacted with $\text{Ca}(\text{HMDS})_2(\text{THF})_2$ in pentane. The solution remains colourless throughout. Once reaction is complete (**1a**: 3 days, **1b** 2 hours) the solvent is removed, and the product extracted in pentane. Pure **1a** and **1b** may be crystallised from cold pentane in good yields (**1a**: 62%; **1b**: 50%).

1a and **1b** represent the first examples of 'PCP' complexes of calcium. Indeed, pincer complexes of Ca are relatively rare.^{20–28} Both give the expected $^{31}\text{P}\{^1\text{H}\}$ NMR signals


Scheme 1 The synthetic route to **1a** and **1b**.

^a Department of Chemistry, Imperial College London, Molecular Sciences Research Hub, 82 Wood Lane, London, UK

^b School of Chemistry, Trinity College Dublin, College Green, Dublin 2, Ireland

† Electronic supplementary information (ESI) available. CCDC 2423347–2423351. For ESI and crystallographic data in CIF or other electronic format see DOI: <https://doi.org/10.1039/d5cc00872g>

‡ Both these authors contributed equally and have permission to represent themselves as first author.



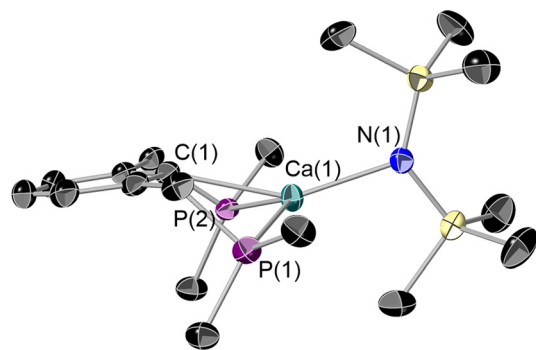


Fig. 1 The single crystal X-ray diffraction structure of **1a**. **1b** is isostructural. Thermal probability ellipsoids at 50%. Hydrogen atoms and the methyl groups of the *tert*-butyl groups are omitted for clarity. Colours: black (carbon), purple (phosphorus), turquoise (calcium), blue (nitrogen), yellow (silicon).

(at δ 24.7 and 122.1 ppm for **1a** and **1b**, respectively). Cyclic voltammetry studies were also undertaken however no electrochemical events were observed, even measuring to -3.0 V (vs. Fc/Fc^+).

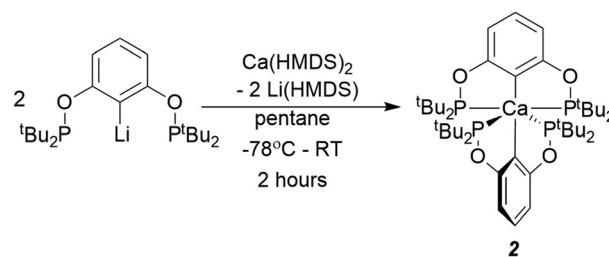
Fig. 1 shows the solid-state X-ray derived structure of **1a**, **1b** is isostructural. The calcium centre is tetracoordinate, and adopts an extremely distorted see-saw geometry; **1b** is slightly closer to a square planar geometry than **1a** (τ_4 parameters 0.572 for **1a**, 0.557 for **1b**).²⁹

1a and **1b** are air- and moisture-sensitive solids, which can be kept at room temperature in a N_2 glovebox. We have not been successful in accessing Ca PCP complexes from CaI_2 , $\text{Ca}(\text{CH}_2\text{Ph})_2(\text{THF})$, $\text{Ca}(\text{OTf})_2$ nor directly from Ca metal. **1a** and **1b** are quite reticent in terms of reactivity. Protonation reactions (with one equivalent of HOTf or Et_3NHCl) resulted in pincer ligand protonation preferentially over amide protonation. Reactions with H_2 and common hydride sources (NaH and NaBH_4) resulted in no reaction, even upon heating.

Reaction of **1b** did occur with NaBET_3H and similar hydride sources (KBET_3H , LiBET_3H , N-selectride). Upon initial addition, three distinct new $^{31}\text{P}\{^1\text{H}\}$ resonances appear, at δ 124 ppm, δ 126 ppm and δ 130 ppm. Upon addition of excess hydride source, the resonance at δ 130 ppm grows to be the sole product. It was posited that the resonances at δ 124 ppm and δ 126 ppm could be the targeted $(^t\text{BuPOCOP})\text{CaH}$ species so attempts were made to isolate these. On one occasion crystallisation from pentane resulted in a crystal suitable for X-ray diffraction which elucidated one of these species to be not the targeted hydride, but instead $(^t\text{BuPOCOP})_2\text{Ca}$ (**2**).

2 can be intentionally made by reacting 2.5 equivalents of $\text{Li}[^t\text{BuPOCOP}]$ with $\text{Ca}(\text{HMDS})_2$ (Scheme 2). Analogous reactions with $\text{Li}[^t\text{BuPCP}]$ were not clean, yielding multiple, unidentified products. Recrystallisation from a pentane solution yields **2** in moderate yields (39%). Changing the alkyl group on the phosphine backbone from *tert*-butyl to *iso*-propyl resulted in the exclusive formation of the homoleptic product $(^i\text{PrPOCOP})_2\text{Ca}$ (**3**) even if a 1 : 1 mixture of Ca and pincer is used.

For both **2** and **3**, the two $^t\text{BuPOCOP}$ ligands are equivalent at room temperature in the solution phase, giving a single broad resonance in the $^{31}\text{P}\{^1\text{H}\}$ NMR (**2**: δ 126 ppm; **3**: δ 113 ppm). The



Scheme 2 The synthesis of **2**.

^1H NMR spectra give the expected resonances, with a single doublet corresponding to the *tert*-butyl protons for **2** (δ 1.21 ppm), and the septet and two apparent doublets of doublets corresponding to the *iso*-propyl protons in **3** (δ 1.93 ppm, δ 1.14 ppm, δ 1.04 ppm respectively). The single crystal X-ray derived structure of **2** is shown in Fig. 2. **3** is isostructural.

For **2**, the calcium centre sits upon a special position (C_2 axis), so that the two POCOP ligands are symmetry related. The binding of the two ligands almost fully encapsulates the calcium centre.

The geometry of the calcium centre is intriguing. Though a six coordinate complex, it does not adopt the expected octahedral coordination. On inspection, it seems that the geometry is entirely driven by the steric encumbrance of the phosphine groups on the ligands. If one only considers these four ligating groups (P(1), P(2), P(1'), P(2')), and ignores the carbon atoms from the arene ring (C(1), C(1')), the structure reveals itself to be approximately tetrahedral. Indeed, using the same treatment on **1a** and **1b** reveals the Ca centre to be adopting a trigonal planar geometry with P(1), P(2) and N(1) (Σ angles around Ca (ignoring C) **1a**: 359.0° ; **1b**: 359.5°).

Some key structural metrics from **1a**, **1b**, **2** and **3** are summarised in Table 1. The Ca–C distances are approximately the same throughout and lie in the range of other structurally characterised Ca–C_{aryl} complexes.³⁰ The bond lengths are significantly longer than the previously characterised Mg PCP

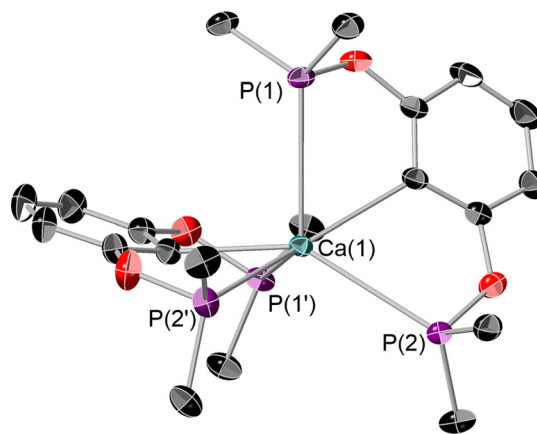


Fig. 2 The single crystal X-ray derived structure of **2**. Thermal ellipsoids at 50% probability, hydrogen atoms and *tert*-butyl methyl groups omitted for clarity. Colours: Red (oxygen) otherwise same as Fig. 1. **3** is isostructural.



Table 1 Selected structural parameters for **1a**, **1b**, **2** and **3**

	1a	1b	2	3
Ca(1)–P(1)	2.9796(6)	2.9439(8)	3.1753(5)	2.966(1)
Ca(1)–P(2)	2.9859(6)	2.9587(7)	3.0653(5)	3.013(1)
Ca(1)–C(1)	2.513(2)	2.516(2)	2.528(2)	2.526(3)
Ca(1)–N(1)	2.285(2)	2.279(2)	n/a	n/a
Ca to C(1)–P(1)–P(2) plane	1.174(2)	0.799(2)	1.420(2)	1.202(3)
P(1)–Ca(1)–P(2)	130.43(1)	130.07(2)	120.00(2)	122.8(1)

complexes, reflecting the increased ionic radius (Mg–P distances (Å) 2.770(1)/2.761(1) for $\text{Mg}^{\text{Me}}\text{PCP}_2$ and 2.692(1)/2.961(1)/2.863(1)/2.689(1) for $\text{Mg}^{\text{Ph}}\text{PCP}_2$).^{18,19} The slight increase in Ca–P bond lengths in **2** compared to **1b** is presumably due to increased steric crowding. Though there are structurally characterised homoleptic $^{\text{R}}\text{PCP}$ complexes, **2** and **3** mark the first homoleptic $^{\text{R}}\text{POCOP}$ complexes.

In most $^{\text{R}}\text{PCP}/^{\text{R}}\text{POCOP}$ pincer complexes the metal centre is ligated by the PCP in an almost perfect meridional fashion. By contrast in our complexes the metal is significantly out of the C(1)–P(1)–P(2) plane, particularly for **1a** and **2**.

In the reaction of **1b** with PhSiH_3 , rather than forming the expected Ca hydride, we found that the silane attached to the ligand instead (presumably with concomitant formation of $^{\text{t}}\text{CaH}(\text{N}(\text{HMDS})_2)$), producing $(^{\text{t}}\text{BuPOCOP})\text{SiH}_2\text{Ph}$, **4** (Scheme 3).

4 can be isolated and crystallised from a pentane solution cooled to -40°C . Its structure is shown in Fig. 3 and it is clear there is no interaction between the silane and the pendant phosphine arms.

A series of density functional theory (DFT) calculations have been carried out to interrogate the nature of bonding in complexes **1a**, **1b**, **2** and **3**. Geometries of all complexes were optimised using the M06L functional in conjunction with the def2-TZVP (Ca, P, N, O) and def2-SVP (C, H) basis sets, giving excellent agreement with their crystallographic counterparts (Table S1, ESI[†]). Detailed analysis of the corresponding wavefunctions obtained from subsequent single point calculations (M06-D3/def2-TZVPP) reveals that for all complexes the HOMO is dominantly localised on the aryl *ipso*-carbon. The significant lone pair character of this centre explains why the observed reaction of **1b** with phenylsilane does not yield the targeted calcium hydride complex (Fig. 4). The LUMO resides on P centres with admixture of 4s and 3d orbital character from Ca^{2+} .

The distorted see-saw geometry around the tetracoordinate calcium centre in both **1a** and **1b** is closely reproduced in the optimised geometries (calculated τ_4 values of 0.55 and 0.60, respectively), although the PES is relatively flat. Structural

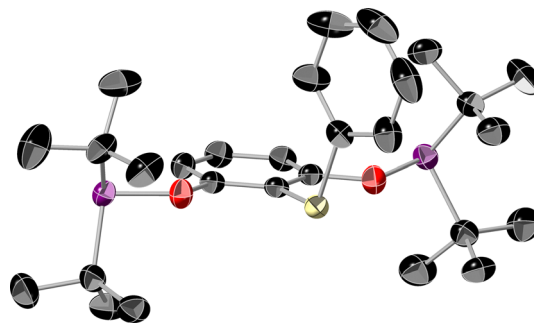


Fig. 3 The single crystal X-ray diffraction structure of **4**. Thermal ellipsoids set at 50% and hydrogen atoms omitted for clarity. Colours as in Fig. 1.

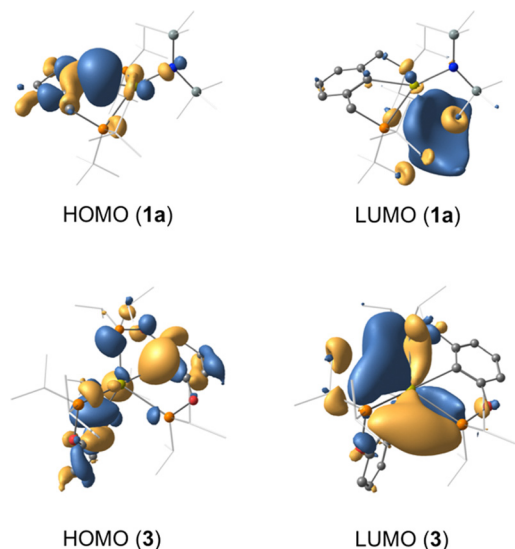
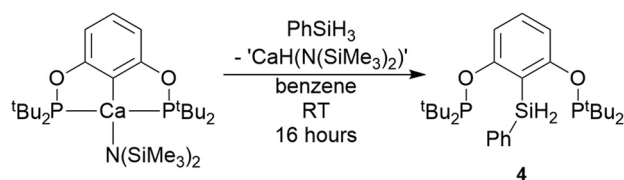


Fig. 4 Highest occupied molecular orbital (HOMO) and lowest unoccupied molecular orbital (LUMO) of complexes **1a** and **3** (isovalue 0.03 a.u.). Hydrogens cloaked for clarity.

isomers of both complexes with enforced square-planar geometries and (near) linear $C_{\text{ipso}}\text{--Ca--N}$ angles are destabilised by $\sim 3 \text{ kcal mol}^{-1}$ relative to the global minimum, both of which relax back to the distorted geometry upon release of the constraints. Similar observations are made for complexes **2** and **3**, for which pseudo-octahedral guess structures reverse back to the experimentally observed distorted geometries upon geometry optimisation.

The presence of non-covalent closed-shell interactions between the calcium centres and the ligands in all complexes was confirmed by analysis of the topology of their total electron densities using quantum theory of atoms in molecules (QTAIM). Linear bond paths between Ca^{2+} and the corresponding donor atoms (P, N and C) are observed for all complexes, approximately coinciding with their respective internuclear bond axes. Bond critical and ring critical points relating to these interactions were readily identified in the molecular graph of each species. The QTAIM descriptors



Scheme 3 The synthesis of $(^{\text{t}}\text{BuPOCOP})\text{SiH}_2\text{Ph}$.



associated with each BCP signal small electron densities, small positive Laplacians and small negative potential energy densities, the latter being approximately matched by the kinetic energy density, *i.e.*, $|G(r)| \approx |V(r)|$. Taken together with small covalent bond orders, these data are characteristic of dative interactions in all species.^{20,31}

The absence of covalent bonding between Ca^{2+} and donor atoms in all complexes is consolidated by intrinsic bond orbitals (IBO) and natural bond orbitals (NBO), underpinning that these interactions are largely due to electron donation from the P, N and C centres with minor contribution from the Ca^{2+} orbital manifold (Fig. S14, ESI[†]). A quantitative measure of the donor–acceptor interactions is obtained from second order perturbation theory of the Fock matrix in the NBO basis, with the vacant 4s orbital of Ca^{2+} serving as the main acceptor orbital. Donations from the P and C lone pairs in complexes **1a** ($E^{(2)} = 12.1\text{--}15.8 \text{ kcal mol}^{-1}$) and **1b** ($E^{(2)} = 14.2\text{--}14.4 \text{ kcal mol}^{-1}$) govern the interactions, while donation from the HMDS ligand are somewhat weaker in both cases ($E^{(2)} = 4.0\text{--}5.0 \text{ kcal mol}^{-1}$). Likewise, in **2** and **3**, the estimates of $E^{(2)}$ for $\text{LP(P)} \rightarrow \text{Ca}^{2+}$ and $\text{LP(C)} \rightarrow \text{Ca}^{2+}$ donations are in the range 9.9–18.2 kcal mol^{-1} . Atomic charges on the calcium ion obtained from both NPA (1.60–1.73) and QTAIM (1.50–1.55) schemes indicate that this centre adopts an oxidation states close to +2 in all complexes.

A series of PCP and POCOP calcium complexes have been made, characterised and their structures investigated by computational calculations. The complexes' geometries are derived predominantly from the steric effects of the phosphine side arms of the pincer ligands. The HOMO of the complexes is the interaction between the aryl-carbon and the calcium centre, which results in the onward reactivity being focused on these atoms, rather than the HMDS ligand.

Data availability

Crystallographic information files (.cif) for all complexes have been deposited in the CCDC (2423347 (**1a**), 2423349 (**1b**), 2423348 (**2**), 2423351 (**3**) and 2423350 (**4**)). Other experimental data in support of this paper are presented in the ESI.[†]

Conflicts of interest

There are no conflicts of interest to declare.

Notes and references

- 1 V. Grignard, *C. R. Hebd. Seances Acad. Sci.*, 1900, **130**, 1322–1324.

- 2 M. Westerhausen, *Coord. Chem. Rev.*, 2008, **252**, 1516–1531.
- 3 M. S. Hill, D. J. Liptrot and C. Weetman, *Chem. Soc. Rev.*, 2016, **45**, 972–988.
- 4 E. Fazekas, P. A. Lowy, M. Abdul Rahman, A. Lykkeberg, Y. Zhou, R. Chamenahalli and J. A. Garden, *Chem. Soc. Rev.*, 2022, **51**, 8793–8814.
- 5 C. Brinkmann, A. G. M. Barrett, M. S. Hill and P. A. Procopiou, *J. Am. Chem. Soc.*, 2012, **134**, 2193–2207.
- 6 J. Escorihuela, A. Lledós and G. Ujaque, *Chem. Rev.*, 2023, **123**, 9139–9203.
- 7 M. Magre, M. Szewczyk and M. Rueping, *Curr. Opin. Green Sustainable Chem.*, 2021, **32**, 100526.
- 8 M. D. Anker, C. E. Kefalidis, Y. Yang, J. Fang, M. S. Hill, M. F. Mahon and L. Maron, *J. Am. Chem. Soc.*, 2017, **139**, 10036–10054.
- 9 S. Brand, H. Elsen, J. Langer, W. A. Donaubauer, F. Hampel and S. Harder, *Angew. Chem., Int. Ed.*, 2018, **57**, 14169–14173.
- 10 B. Rösch, T. X. Gentner, J. Langer, C. Färber, J. Eyselein, L. Zhao, C. Ding, G. Frenking and S. Harder, *Science*, 2021, **371**, 1125–1128.
- 11 Y. Liang, U. K. Das, J. Luo, Y. Diskin-Posner, L. Avram and D. Milstein, *J. Am. Chem. Soc.*, 2022, **144**, 19115–19126.
- 12 M. H. Chisholm, J. C. Gallucci and K. Phomphrai, *Inorg. Chem.*, 2004, **43**, 6717–6725.
- 13 S. Harder, *Chem. Rev.*, 2010, **110**, 3852–3876.
- 14 B. Rösch and S. Harder, *Chem. Commun.*, 2021, **57**, 9354–9365.
- 15 Y. C. Tsai, *Coord. Chem. Rev.*, 2012, **256**, 722–758.
- 16 B. Stadler, H. H. Y. Meng, S. Belazregue, L. Webster, A. Collauto, K. M. Byrne, T. Krämer and F. M. Chadwick, *Organometallics*, 2023, **42**, 1278–1285.
- 17 L. Webster, T. Krämer and F. M. Chadwick, *Dalton Trans.*, 2022, **51**, 16714–16722.
- 18 A. Koch, S. Kriek, H. Görls and M. Westerhausen, *Inorganics*, 2016, **4**, 39.
- 19 A. Pape, M. Lutz and G. Müller, *Angew. Chem., Int. Ed. Engl.*, 1994, **33**, 2281–2284.
- 20 Y. Liang, I. Efremenko, Y. Diskin-Posner, L. Avram and D. Milstein, *Angew. Chem., Int. Ed.*, 2024, **63**, e202401702.
- 21 M. Arrowsmith, M. S. Hill and G. Kociok-Köhn, *Organometallics*, 2010, **29**, 4203–4206.
- 22 A. Koch, S. Kriek, H. Görls and M. Westerhausen, *Organometallics*, 2017, **36**, 994–1000.
- 23 J. Jenter, R. Köppe and P. W. Roesky, *Organometallics*, 2011, **30**, 1404–1413.
- 24 M. J. C. Dawkins, A. N. Simonov and C. Jones, *Dalton Trans.*, 2020, **49**, 6627–6634.
- 25 P. S. Kubiak, A. L. Johnson, P. J. Cameron and G. Kociok-Köhn, *Eur. J. Inorg. Chem.*, 2019, 3962–3969.
- 26 J. Langer, M. Köhler, H. Görls and M. Westerhausen, *Chem. – Eur. J.*, 2014, **20**, 3154–3161.
- 27 A. Koch, Q. Dufrois, M. Wirgenings, H. Görls, S. Kriek, M. Etienne, G. Pohnert and M. Westerhausen, *Chem. – Eur. J.*, 2018, **24**, 16840–16850.
- 28 J. A. Darr, S. R. Drake, D. J. Otway, S. A. S. Miller, D. M. P. Mingos, I. Baxter, M. B. Hursthouse and K. M. A. Malik, *Polyhedron*, 1997, **16**, 2581–2588.
- 29 L. Yang, D. R. Powell and R. P. Houser, *Dalton Trans.*, 2007, 955–964.
- 30 A. Koch, S. Kriek, H. Görls and M. Westerhausen, *Organometallics*, 2017, **36**, 2811–2817.
- 31 C. Lepetit, P. Fau, K. Fajerweg, M. L. Kahn and B. Silvi, *Coord. Chem. Rev.*, 2017, **345**, 150–181.

